

EVOLUTION OF RELATIVISTIC PLASMA WAVE-FRONT IN LWFA*

F. Fang, C.E. Clayton, K.A. Marsh, A.E. Pak, J.E. Ralph and C. Joshi
 EE Department, University of California at Los Angeles, Los Angeles, CA, 90095
 N.C. Lopes, Grupo de Lasers e Plasmas, Instituto Superior Técnico, Lisbon

Abstract

In a laser wakefield accelerator experiment where the length of the pump laser pulse is several plasma period long, the leading edge of the laser pulse undergoes frequency downshifting as the laser energy is transferred to the wake. Therefore, after some propagation distance, the group velocity of the leading edge of the pump pulse—and therefore of the driven electron plasma wave—will slow down. This can have implications for the dephasing length of the accelerated electrons and therefore needs to be understood experimentally. We have carried out an experimental investigation where we have measured the velocity v_f of the 'wave-front' of the plasma wave driven by a nominally 50fs (FWHM), intense ($a_0 \sim 1$), $0.8\mu\text{m}$ laser pulse. To determine the speed of the wave front, time- and space-resolved shadowgraphy, interferometry, and Thomson scattering were used. Although low density data ($n_e \sim 1.3 \times 10^{19}\text{cm}^{-3}$) showed no significant changes in v_f over 1.5mm (and no accelerated electrons), high-density data shows accelerated electrons and an approximately 5% drop in v_f after a propagation distance of about $800\mu\text{m}$.

INTRODUCTION

In the laser wake field accelerator (LWFA) scheme, as a high intensity ($\geq\text{TW}$) short (sub ps) laser pulse propagates into a plasma, it drives a plasma wake. The electric field of this plasma wave can trap and accelerate electrons. This idea was first proposed by Tajima and Dawson in 1979[1]. In early experiments and up to as recently as 2002, the maximum energy gain was on the order of 100 MeV with a continuous energy spectrum (see, for example, Ref. [2]). As laser technology improved, eventually 'quasi-mono-energetic' electron were produced in either a neutral gas jet or a preformed plasma channel [3, 4, 5] with energies in excess of 100 MeV. Because its high field and compact size, laser-wakefield-based accelerators are potentially replacements for more traditional linacs in the areas of high-energy physics as well as medical, industrial, and research applications.

Although quasi-mono-energetic electron beams have been seen in several LWFA experiments [3, 4, 5], the physical processes of electron trapping, acceleration, and eventual dephasing are still not well understood. Simulation and theoretical work [6, 7, 8, 9] suggests, that after the laser pulse propagates into a plasma, it quickly undergoes self-focusing and longitudinal compression where it is sufficiently intense and short enough to access the so-called

'blow-out' or 'bubble' regime. In this regime, the electrons are expelled mostly radially by the ponderomotive force of the laser leaving behind a bubble of ions. The space-charge force of these ions pulls the expelled electrons, now in a sheath around the ion bubble, back toward the axis where a majority of them overshoot and set up a 3-dimensional wake. However, some of the electrons on the inside of the sheath will gain sufficient longitudinal momentum to be trapped and accelerated to velocities $> v_f$. Simulations show that this trapping process can occur in the first few buckets. It is believed that, if a sufficient number of electrons are trapped, then the space-charge of *these* electrons will suppress further trapping and lead to an observed quasi-mono-energetic electron bunch if the plasma length is close to the dephasing length. In calculating the classical dephasing length, it is assumed that the velocity of the wake does not change during this dephasing process. However, it is known that frequency-changes in the laser pulse, as well as pulse-envelope changes due to diffraction and focusing, will lead to a change in the group velocity of the laser pulse and thus to the velocity of the wake. Since very small changes in this group velocity v_g can make large changes in the Lorentz factor γ_{ph} associated with the phase velocity v_{ph} of the wake, small v_g changes can have profound effects on the trapping, dephasing, and ultimately, the observed maximum electron energy. These continuous and subtle changes in the wake velocity have not been experimentally observed to our knowledge.

In this paper, we attempted to quantify changes in v_{ph} by measuring an equivalent physical parameter: the effect of the density depression/compression in the first few bubbles on a short probe beam. We use this probe beam for time- and space-resolved shadowgraphy, interferometry, and Thomson scattering. The v_{ph} changes are too small to be measured at a relatively low density of $1.3 \times 10^{19}\text{cm}^{-3}$. Thus this density can be used as a calibration or benchmark for the diagnostics. Applying the same diagnostics to a high density ($5 \times 10^{19}\text{cm}^{-3}$) plasma, we are able to observe these small velocity changes. The purpose of this paper is to describe how these diagnostics are applied to the these experiments. The details of the physics inferred from the data will be published elsewhere.

EXPERIMENTS AT LOW DENSITY

The experimental setup for the low density experiment is shown in Fig. 1. A 2 TW, Ti:Sapphire laser pulse with a length of 50fs, is split by a beam-splitter into two parts: 99% is reflected for the pump beam while the transmitted pulse is used as the probe beam. The pump beam is focused

* Work supported by DOE Grant Nos. DE-FG52-03NA00138 and DE-FG02-92ER40727 and Grant POCI/FIS/58776/2004 (FCT-Portugal)

onto the gas-jet entrance with an off-axis parabolic mirror (OAP) to a spot size $10\mu\text{m}$. The helium gas jet is about 1.5 mm long with a uniform density of $1.3 \times 10^{19}\text{cm}^{-3}$, measured by a Mach-Zehnder interferometer. After dumping 95% of the transmitted pump beam by a 800nm broadband-coated beam-splitter, the remaining pump light is collected and imaged onto the slit of a spectrograph for measuring the forward scattered (FS) spectrum. The probe beam, after an adjustable delay, is sent to the gas jet with an angle \sim orthogonal to the pump beam. As shown in Fig. 1, the two lenses downstream of the probe beam are used to image the gas-jet plane onto camera1 after reflection by a beam-splitter (BS). This is the shadowgraph (SDG) diagnostic. On the transmission side of the BS, there is a short-focal-length lens (located after the gas-jet image plane) to focus the probe beam to the front edge of a gold mirror as in a Lloyd-mirror interferometer[10]. This mirror reflects the 'reference beam' (the part of the probe beam that does not go through gas jet) and overlaps it with the 'scene beam'. This is the part that *does* go through the gas jet and contains information on the refractive index variation in the plasma (see heavy magenta lines in Fig. 1). The image of the gas jet is reformed on camera2 within an interference pattern. This is the interferometry diagnostic (INF). The refractive index in a plasma is $n \simeq 1 - \frac{n_e}{2n_{cr}}$, where n_e is the plasma electron density, $n_{cr} = \frac{\epsilon_0 m \omega^2}{e^2}$ is the critical density, and ω_0 is the laser frequency. Therefore, any on-axis depression in n_e acts as a cylindrical lens for the probe beam while the channel sheath acts as a negative lens. The inset in Fig. 1 shows one example each of SDG and INF. The spatial resolution of the SDG image is estimated to be $24\mu\text{m}$; i.e., \gg the laser spot size.

The well-defined, bright stripe comprising the SDG image is consistent with this view of the on-axis n_e depression acting as a focusing, cylindrical lens. This same on-axis enhancement of the probe beam intensity can also be seen in the INF image. Here, the fringe spacing is about $65\mu\text{m}$ and the inferred peak n_e (after Abel inversion) is about $1.3 \times 10^{19}\text{cm}^{-3}$. Note that the fringes in the INF suggest that the plasma formation occurs slightly ($\leq 50\mu\text{m}$) ahead of the leading edge of the SDG image (see the two large black arrows in Fig. 1). We believe that the well-defined leading edge seen in the SDG image is the 'plasma wave-front'; that is, the perturbation to the refractive index due to the wakefield, integrated over the transit time convolved with the pulse length of the probe beam. On the other hand, the leading edge or first shifted fringe in the INF occurs when the laser intensity exceeds the tunneling-ionization thresholds for He-I (He-II) at $\sim 10^{15}\text{W}/\text{cm}^2$ ($\sim 10^{16}\text{W}/\text{cm}^2$). Thus, this diagnostic measures the location of the 'ionization front'. Note that this slight offset in the apparent longitudinal position of the plasma wave-front relative to the ionization front is consistent with ionization occurring before wake formation. Time evolutions of the plasma wave-front and ionization front were obtained by recording SDG and INF images with delay line steps of

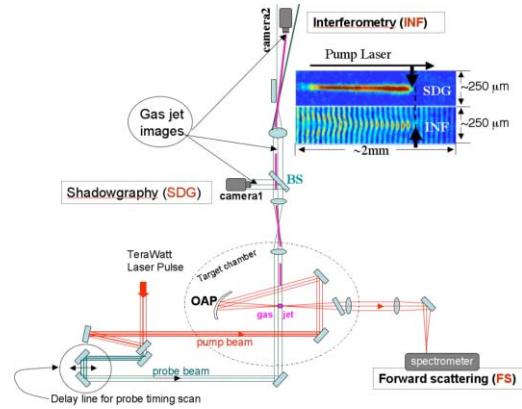


Figure 1: Schematic of the low density experimental set up. The two images shown are examples of the SDG (top) and INF (bottom). The pump travels from left to right. The position of the fronts for these example images is about 1.2mm into the jet.

333fs. A selection of the resulting images are shown in in Fig. 2(a). The delay time labeled 'zero' corresponds to the case where the probe pulse and the pump pulse overlap in time at the entrance to the gas jet. The blue circles (green diamonds) in Figure 2(b) show the longitudinal position of the plasma wave-front (ionization front) while the red line is the linear v_{gr} of the pump beam for a uniform plasma of $n_e = 1.3 \times 10^{19}\text{cm}^{-3}$. The shot-to-shot variation in the data are thought to be due to real variations in the incoming pump pulse and/or in the initial profile of the He-gas from the jet. Additionally, due to the discreteness of the fringes, there are inherent uncertainties as to where the ionization front actually begins. To the extent that the data for the position of these fronts follow the red line, we may conclude that, at this low n_e , the pump propagates with no substantial distortion of its envelope or spectrum all the way to $\sim 1.5\text{mm}$, the end of the gas jet. In fact, the maximum measured shift in FS was substantially less than the pump-laser bandwidth of $\sim 24\text{nm}$ and no accelerated electrons were observed. When we go to the high-density gas jet, the limited collection angle for the probe beam will render the interferometry essentially useless. However, as we will see, the apparent focusing effect of the density depression at the very front of the shadowgraphy will more than compensate for this strong probe-beam diffraction.

EXPERIMENTS AT HIGH DENSITY

The high-density experiments were carried out with a 2mm-long, He gas jet giving $n_e \sim 5 \times 10^{19}\text{cm}^{-3}$. The experimental set up is shown in Fig. 3. In addition to the SDG and FS diagnostics, we added spatially-resolved, transverse Thomson scattering (TS). The transmitted probe beam is collected to give an SDG image, as described before. For TS k-matching, the probe beam was set to an angle of 96° to the pump beam and was focused to overlap with the plasma with an elliptical spot of $\sim 50\mu\text{m}$ tall by 3mm wide.

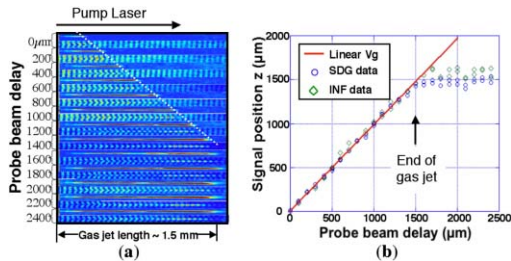


Figure 2: (a) Selected SDG and INF image pairs. The arrows in Fig. 1 show more clearly the front-positions to be plotted in (b). The dashed line is a guide for the eye. (b) Experimental results for SDG (blue circles) and INF (green diamonds) of the probe timing scan (333fs steps) along with the laser linear v_{gr} (red line).

The calculated TS angle is 9° . These photons were collected with a lens, rotated 90° , and imaged onto the slit of a imaging-spectrograph. Note, at this high n_e , the temporal duration of the probe beam is long enough to overlap with > 3 plasma wavelengths and the strong radial-component of the plasma wave allows for k-matching. An example of a TS spectrum is shown in the inset (upper right) to Fig. 3. This typical TS spectrum is centered at about 700nm with a bandwidth of typically 40nm. The spatial resolution here is about $50\mu m$. An example of a high-plasma-density SDG image is also shown (upper left in Fig. 3). Note the bright spot at the very front of this SDG image. The vertical size of this feature is probably resolution ($\sim 24\mu m$) limited.

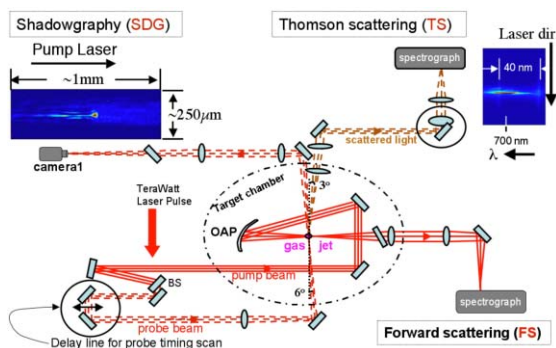


Figure 3: Schematic of the high density set up. The two images are examples of SDG (left) and TS (right).

Figure 4 shows the result of a probe-beam timing scan. This timing scan begins with the probe pulse temporally overlapping the pump pulse at the entrance of the gas jet and ends 1.2mm into the gas jet with a step size of 67fs ($20\mu m$). Some selected TS and SDG images are shown side-by-side in Figure 4(a) and (b). The probe beam delays for these are labeled on the left. From data plotted in Fig. 4(c), one can see that, in contrast to the low n_e case of Fig. 2(b), the velocity of both the plasma wave front and the extreme front-edge of the TS begin to depart from the linear v_g beyond about $300\mu m$ into the plasma. At $800\mu m$ into the plasma, the measured drop in these velocities (the

slope of the plotted data) is about 5 percent which represents about a 40 micron slippage of these fronts relative to v_g . Results from the FS diagnostic (not shown) reveal considerably wings on the red side (much larger than those on the blue side). Results from the electron spectrometer diagnostic (not shown) indicate electrons out to about 40 MeV and often appeared to be quasi-mono-energetic. With the dipole magnet of the electron spectrometer off, some shots showed forward emitted electrons that were extremely well collimated (< 5 mrad full angle).

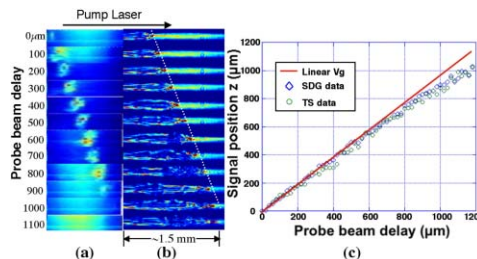


Figure 4: (a) Selected TS images; (b) the corresponding SDG images. The dashed line in (b) is representative of the position of a plasma wave front for the small-delay shots; (c) positions of the TS (green dots) and SDG (blue diamonds) for all images, 67fs steps. The red line in (c) is the linear v_{gr} for a uniform plasma at this n_e .

CONCLUSIONS

In this paper, we used three time- and space-resolved diagnostics; shadowgraph, interferometry, and Thomson scattering to measure the velocity of the plasma wave-front. We found in a low plasma density ($1.3 \times 10^{19} \text{cm}^{-3}$) experiment that the plasma wave-front moved with a constant velocity, equal (within the experimental uncertainty) to the linear laser group velocity, all the way to the end of the 1.5mm gas jet. In a high plasma density ($5 \times 10^{19} \text{cm}^{-3}$) experiment, there is a $\sim 5\%$ drop in the velocity of the plasma wave-front at a distance of $\sim 800\mu m$ into the jet. The slippage of the wave-front relative to a light-speed particle accumulates to about $40\mu m$ at $800\mu m$. Since this is about eight plasma wavelengths, the implications for electron dephasing is clearly of interest.

REFERENCES

- [1] T. Tajima et al., Phys. Rev. Lett. 43, 267270 (1979).
- [2] V. Malka et al, Science 298, 15961600(2002).
- [3] J. Faure et al, Nature 431, 541544(2004).
- [4] C. G. R. Geddes et al, Nature 431, 538541(2004).
- [5] S. P. D. Mangles et al, Nature 431, 535538(2004).
- [6] W. Lu et al, Phys. Rev. Lett. 96, 165002(2006).
- [7] W. Lu et al, Phys. Plasma 13, 056709(2006).
- [8] F. S. Tsung et al, Phys. Plasma 13, 056708(2006).
- [9] I. Kostyukov et al, Phys. Plasma 11, 52565264(2004).
- [10] E. Hecht, Optics 98, 391(1998).